Paper 115

Proceedings of the Eighth International Conference
on Engineering Computational Technology,
B.H.V. Topping, (Editor),
Civil-Comp Press, Stirlingshire, Scotland

Numerical Modelling of Engineering Structures subjected to Dynamic Seismic Loading

S.N. Polukoshko[1], V.F. Gonca[2] and E.V. Uspenska[2]
[1] Engineering Research Institute
"Ventspils International Radio Astronomy Centre"
Ventspils University College, Latvia
[2] Institute of Mechanics, Riga Technical University, Latvia

Abstract

The results of numerical modelling the behaviour of a five-storey building, retaining wall and river embankment in seismic conditions are presented in this paper. Analysis was executed by means of the dynamic module of the Plaxis-8v program, based on the finite element method. Accelerations, velocities and displacements of the control points on the construction and soil are determined; diagrams of internal forces in structural elements are shown. The dependence of the magnitude of internal forces on the assumed model of the soil is found.

Keywords: seismic load, Plaxis, soil models, Rayleigh damping, soil-structure interaction, numerical modelling.

1 Introduction

Problem of dynamic interaction of the construction with the basement soil is very important for dynamics and seismic resistance of structures. It is known that dynamic characteristics of structure and, consequently, its response on dynamic action significantly depend on sub-soil properties [1], [2], [3].

In this work the results of numerical modeling of behavior of engineering construction under action of seismic loading are presented. The modelling was executed with help of dynamic module of Plaxis - 2Dv8 program (Delft, the Netherlands). Plaxis is the finite element code for the analysis in geotechnical engineering. Plaxis-2Dv8 program enables to take into account soil - structure interaction, to use different models of soils (both linear and nonlinear) and to apply different surface configuration and different soil layers inclination [4]. Most of this features are absent in another programs. In dynamic module of Plaxis special boundary conditions are used in order to absorb waves, reaching the boundaries.

The purpose of this work is to understand the effect of parameters of soil model on the earthquake response of structure. For this aim three soil models is compared:

simple linear-elastic body (LE), well-known elastic-perfectly plastic Mohr – Coulomb model (MC) and advanced nonlinear model of hardening soil with stress dependent on soil stiffness (HS). This three types of models, describing the behaviour of the same soil, requiree knowledge of revised values of soil properties with the increasing the complexity of the model.

- Linear elastic model involves two parameters: Young's modulus *E,* Poisson ratio *v*, and represent Hooke's low if isotropic plasticity.
- Linear elastic – perfectly plastic Mohr-Coulomb model requires five parameters: Young's modulus *E,* Poisson ratio *v*, cohesion *c*, friction angle φ and dilatancy angle ψ.
- Hardening soil is elasto-plastic type of hyperbolic model, involving compression hardening to simulate irreversible compression of soil under primary compression. It require besides of parameters *c*, φ and ψ (according to the MC model) basic stiffness parameters: power stress-level dependency of stiffness *m*, secant stiffness in standard drained triaxial test E^{ref}_{50} , tangent stiffness for primary odometer loading E_{oed}^{ref}, unloading/reloading stiffness E_{ur}^{ref} .

The wave velocities *Vp* and *Vs* are calculated related to the stiffness parameters *E* and *v* for each model.

Three types of engineering constructions subject to an earthquake: multy-storey building and retaining wall and river embankment are investigated.

2 Scientific background

The basic equation for the time-dependent movement of a volume under the influence of a dynamic load is:

$$\boldsymbol{M}\underline{\ddot{u}} + \mathbf{C}\underline{\dot{u}} + \mathbf{K}\,\underline{u} = \boldsymbol{F} \tag{1}$$

where: ***M*** - the mass matrix (soil, water and construction), ***C*** - the damping matrix, K – the stiffness matrix, ***F*** – the load vector, $\underline{u}, \underline{\dot{u}}, \underline{\ddot{u}}$ - displacement, velocity and acceleration vectors [4]. Here the theory is described on the base of linear elasticity. However, all models in Plaxis can be used for dynamic analysis. The matrix ***C*** represents the material damping, which is caused by viscous properties, friction or by the development of plasticity. If elasticity is assumed, damping can still be taken into account using the matrix ***C***. In finite element formulations, ***C*** is often formulated as a function of mass and stiffness matrices (Rayleigh damping) as:

$$\boldsymbol{C} = \alpha_R \boldsymbol{M} + \beta_R \boldsymbol{K} \tag{2}$$

This limits the determination of damping matrix to the Rayleigh coefficient α_R and β_R. Here, when the contribution of ***M*** is dominant, more of low frequency vibrations are damped, and when the contribution of ***K*** is dominant more of high-frequency vibrations are damped. Liquefaction of soil is not considered in Plaxis Dynamics. A water-saturated porous soil can bring in the viscous damping on high-frequencies.

3 Numerical examples of computation

In this paper we consider the extended structures: multi-storey building and geotechnical structures (retaining wall and dam) under the action of seismic loads. Length of this structures is much large than its width. The earthquake is also supposed to have a dominant effect across the width of the building; hence, a plane strain analysis which is available in dynamic model of Plaxis Professional Version 8 can be performed. Plane strain does not include the geometric damping; therefore it is necessary to include material damping. Physical damping in the building and the subsoil is simulated by means of Rayleigh damping.

The geometry of studied objects is modelled with a plane strain model; the finite element mesh is based on 15- node elements.The vertical boundaries are taken relatively far away from the building. At the vertical and horizontal boundaries standard earthquake boundary conditions are applied to absorb outgoing waves.

In earthquake problem the dynamic loading source is usually applied along the bottom of the model resulting to shear wave that propagate upwards.

The earthquake is modeled by imposing a prescribed displacement at the bottom boundary. A real accelerogram of an earthquake recorded by U. S. Geological Survey (USGS) in 1989 is used for the analysis; it is taken from the Paxis-v8 library.

3.1 Seismic action on 5-storey building

In this part the five-storey building when subjected to an earthquake is discussed.

The building consists of 5 floors and a basement. It is 12 m wide and 48m length. The total height from the ground level is 5x3m=15 m and the basement is 2 m depth. The dead load and a percentage of the live load acting on each floor are added up, mounting up to 5 kN/m^2. This value is taken as weight of the floors and walls.

The subsoil consists of relatively soft soil layer of 20 m thickness without water, overlaying a rock formation, which is not included in the model. The building itself is composed of 5-noded plate elements. In Fig. 1 the geometry including contact soil massive 112 m in length and 20m in depth and finite element mesh are presented.

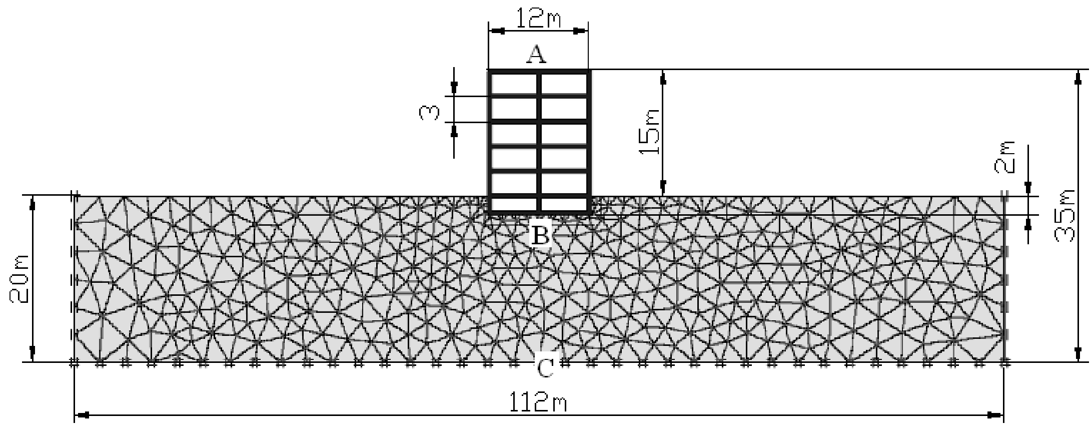

Figure 1: Finite element mesh and geometry of building.

Control points A, B, C are located on the top of building, in the bottom of basement and in the bottom of mesh. Geotechnical soil parameters are given in table 1, material properties of the building - in table 2.

Parameter	Unit	Name	Sand	Sand	Sand
Material model	-		LE	MC	HS
Unit weight above p.l.	kN/m^3	γ_{unsat}	17	17	17
Young's modulus	kN/m^2	E	30000	30000	
Stiffnesss parameters	kN/m^2	E^{ref}_{50}			30000
	kN/m^2	E_{oed}^{ref}	-	-	30000
	kN/m^2	E_{ur}^{ref}	-	-	60000
Power	-	m	-	-	0.5
Poisson's ratio	-	ν	0.2	0.2	0.2
Cohesion	kN/m^2	c_{ref}	-	0.5	0.5
Friction angle	o	φ	-	30	30
Dilatancy angle	o	ψ	-	0	0
Rayleigh damping	-	α_R, β_R	0.01	0.01	0.01

Table 1: Material properties of the subsoil

Parameter	Unit	Name	Floors/ walls	Basement	Middle wall
Material model	-	model	elastic	elastic	elastic
Normal stiffness	kN/m	EA	$5 \cdot 10^6$	$9 \cdot 10^6$	$7.5 \cdot 10^6$
Flexural rigidity	kNm^2/m	EJ	9000	67500	12000
weight	kN/m/m	w	5	10	8
Poisson's ratio	-	ν	0	0	0
Rayleigh damping	-	α_R and β_R	0.01	0.01	0.01

Table 2.Material properties of the building

In the table 3maximum values of vibration parameters of control points are given – maximal horizontal displacement and maximal acceleration for all soil model and the time of this event from the beginning of earthquake is indicated.

Soil model	A				B				C			
	Displace-ment		Accelera-tion		Displase-ment		Accelera-tion		Displase-ment		Accelera-tion	
	u_{max} mm	t, s	a_{max} ms^{-2}	t, s	u_{max} mm	t, s	a_{max} ms^{-2}	t, s	u_{max} mm	t, s	a_{max} ms^{-2}	t, s
LE	54	4.84	1.98	2.92	40	4.56	1.52	2.80	37	4.84	1.76	2.36
MC	55	4.84	1.97	2.92	40	4.56	1.52	2.80	37	4.84	1.76	2.36
HS	51	4.84	2.31	2.88	38	5.04	1.93	2.40	37	4.84	1.76	2.36

Table 3. Maximal parameters of vibration in control points A, B, C

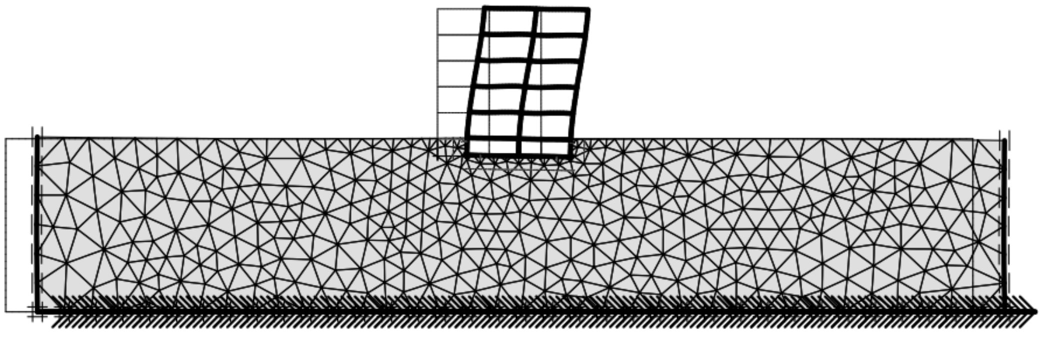

Figure 2: Deformed mesh at t=4.84s, maximum horizontal deformation 54 mm

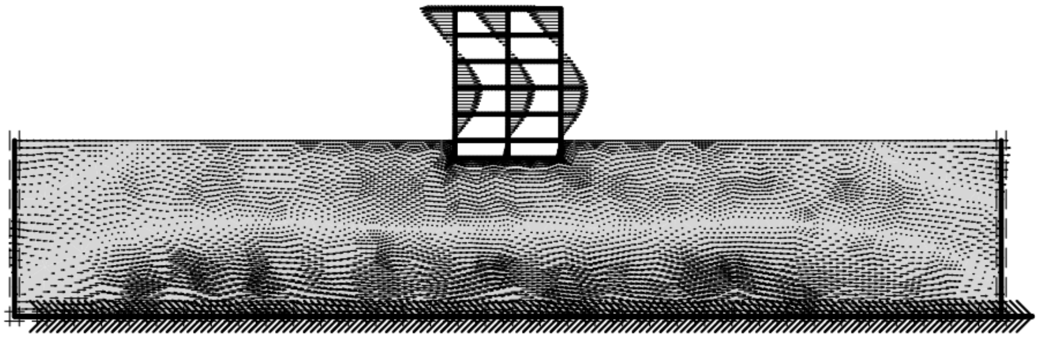

Figure 3: Horizontal acceleration at t=2.92s, maximum value at top 1.98 m/s^2

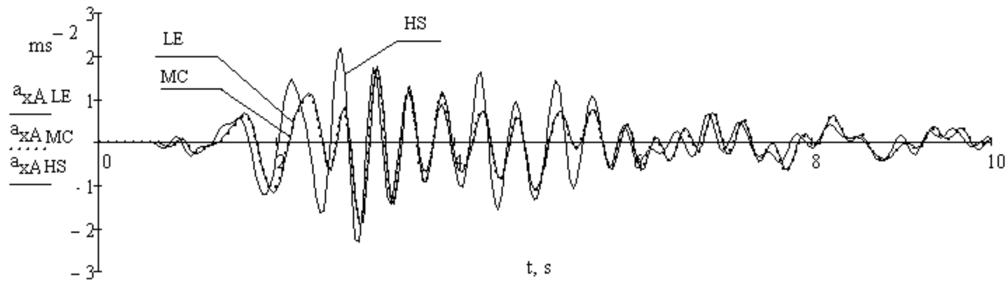

Figure 4: Time-acceleration curve for top of building (point A) in the case of LE, MC and HS soil models

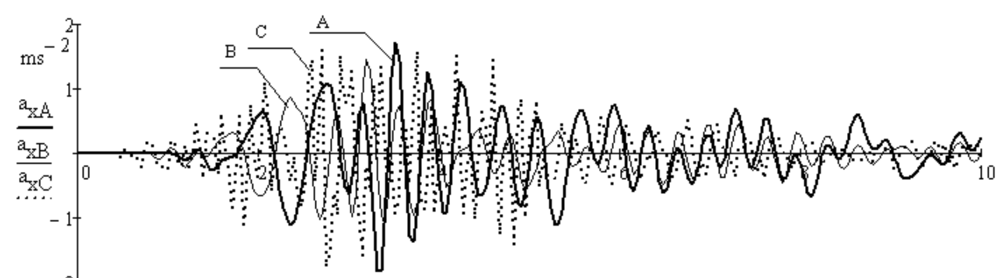

Figure 5: Time-acceleration curve for top of building (point A), basement (point B) and for the mesh bottom (point C) in the case of MC soil model

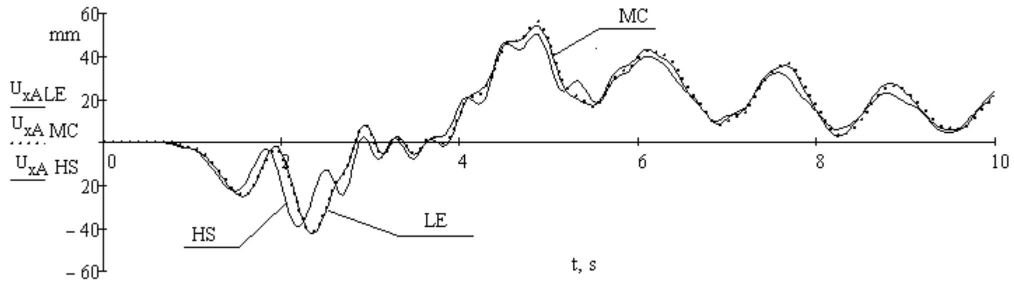

Figure 6: Time-displacement curve for top of building (point A) in the case of LE, MC and HS models

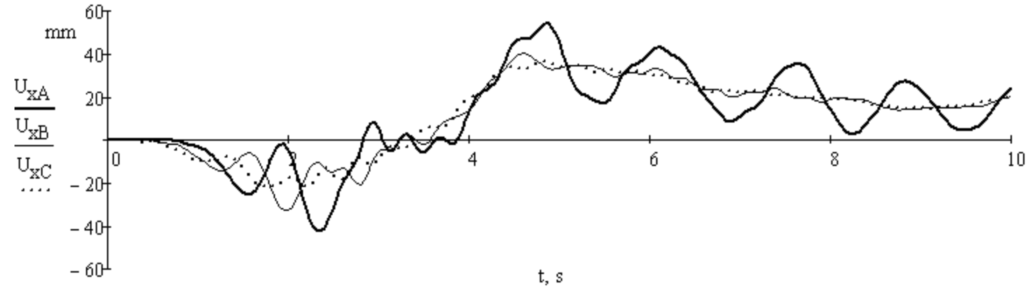

Figure 7: Time-displacement curve for top of building (point A), basement (point B) and for the mesh bottom (point C) in the case MC soil model

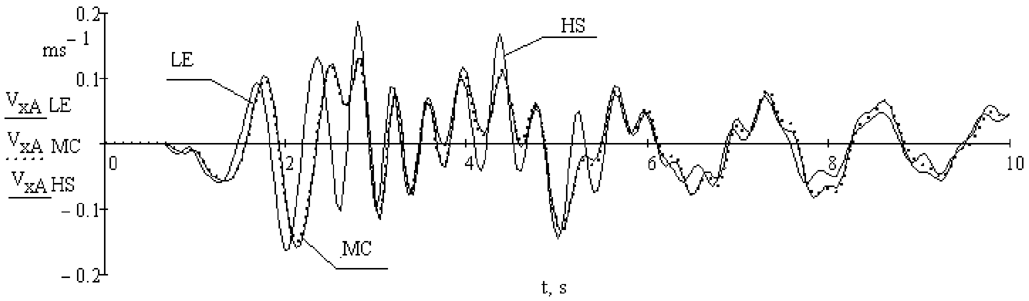

Figure 8: Time-velocity curve for top of building (point A) in the case of LE, MC and HS models

Fig. 2 shows the deformed mesh and maximum horizontal deformation at the top of building, Fig 3 – maximum horizontal acceleration of the top for LE model.
In Fig. 4 time - acceleration curves for the top of building are shown for every type of models, in Fig 5 time - acceleration curves for control points of MC soil model.
In Fig. 6 time-displacement curves and in Fig. 8 time-velocity curves are presented for point A at the top of building for all types of soil models. Plots in Fig. 7 show time-displacement curves for control points A, B, C for all types of soil models.
Fig. 9,11,12 show the envelopes of bending moments curves in case of LE, MC and HS soil model. Bending moments in frame differ a little, bending moments in the basement slab don't differ, but bending moments in basement wall differ larger.

It is connected with the fact of basement rigidity, in the case of flexible basement constructions bending moments differ significantly.

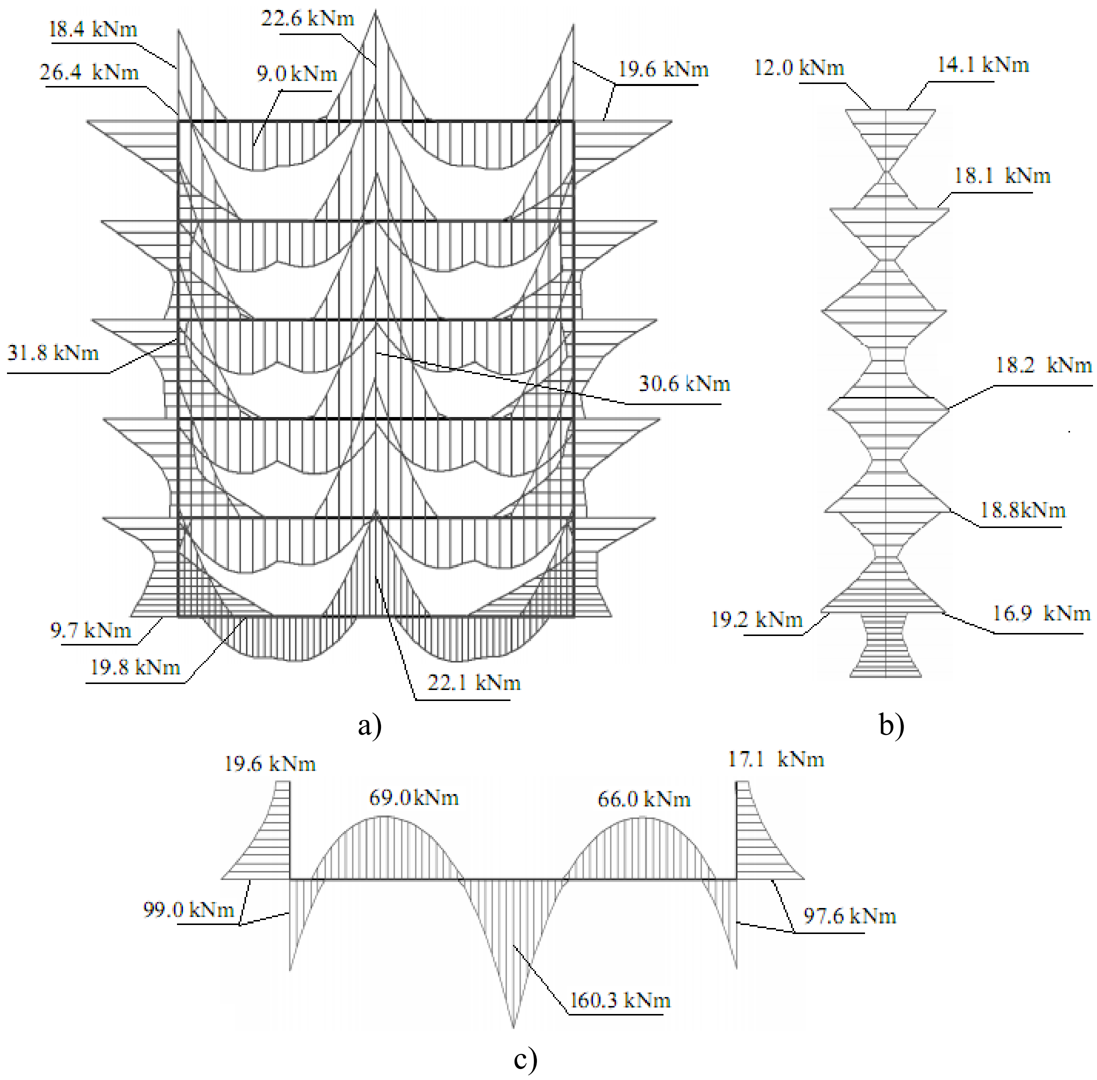

Figure 9: Plot of envelopes of bending moment in case of LE soil model:
a – in frame, b-in middle wall, c – in basement

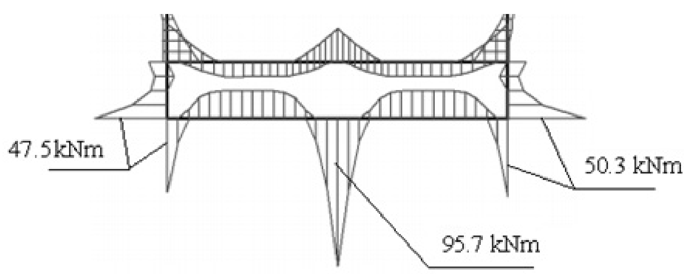

Figure 10: Plot of envelopes of bending moment in flexible basement for LE model

The examples of envelops of bending moments in basement with normal stiffness and flexural rigidity the same as floors/walls construction (tab. 2) are given in Fig. 10,12,14.

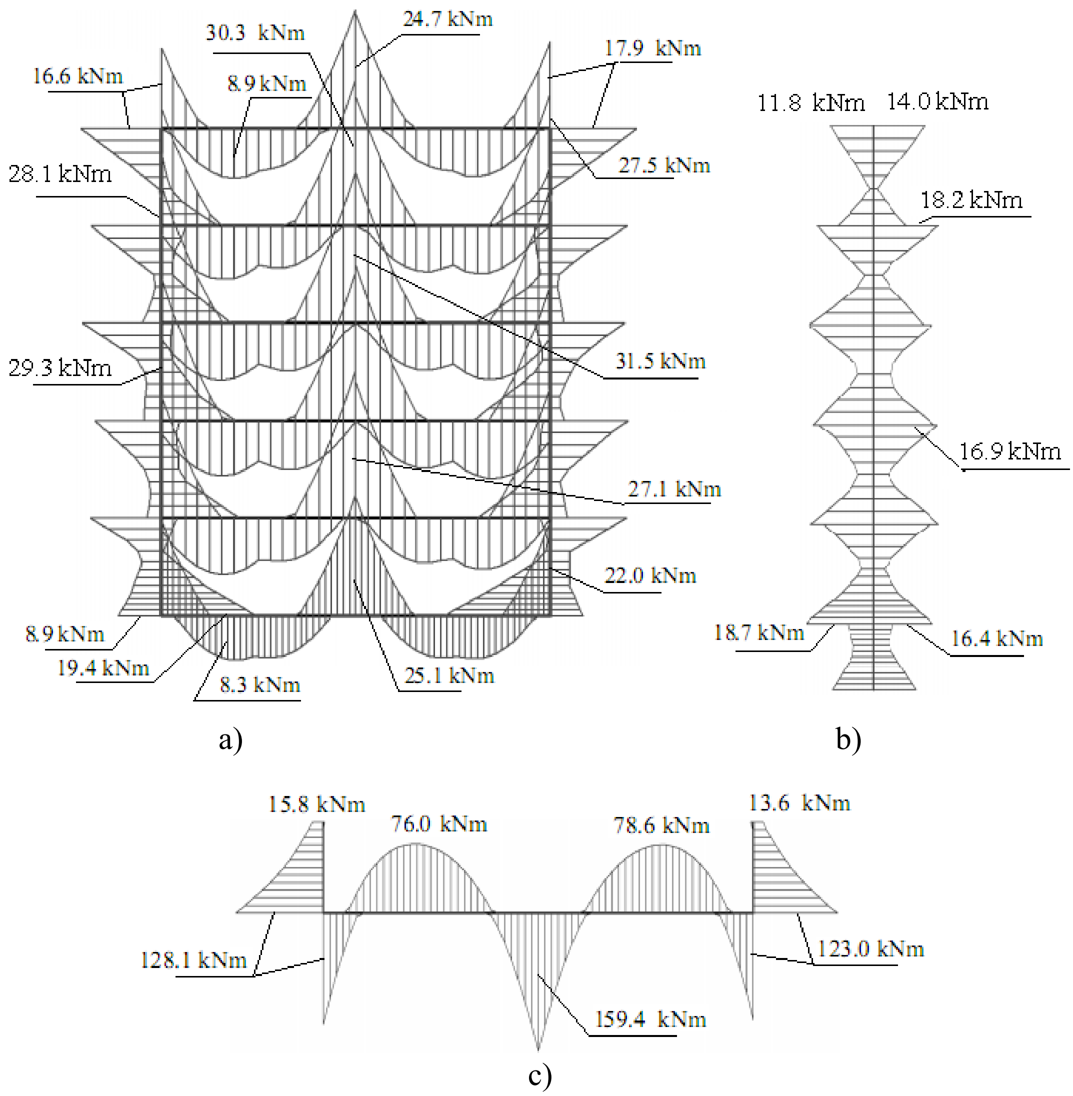

Figure 11: Plot of envelopes of bending moment in case of MC soil model: a – in frame, b-in middle wall, c – in basement

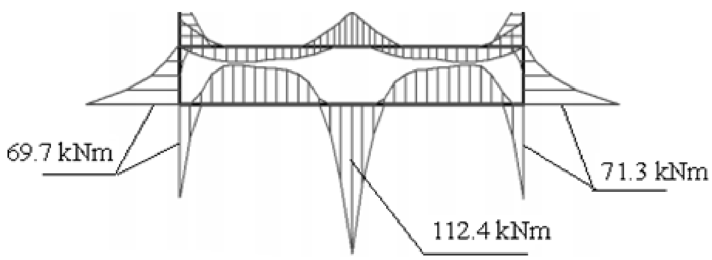

Figure 12: Plot of envelopes of bending moment in flexible basement for MC model

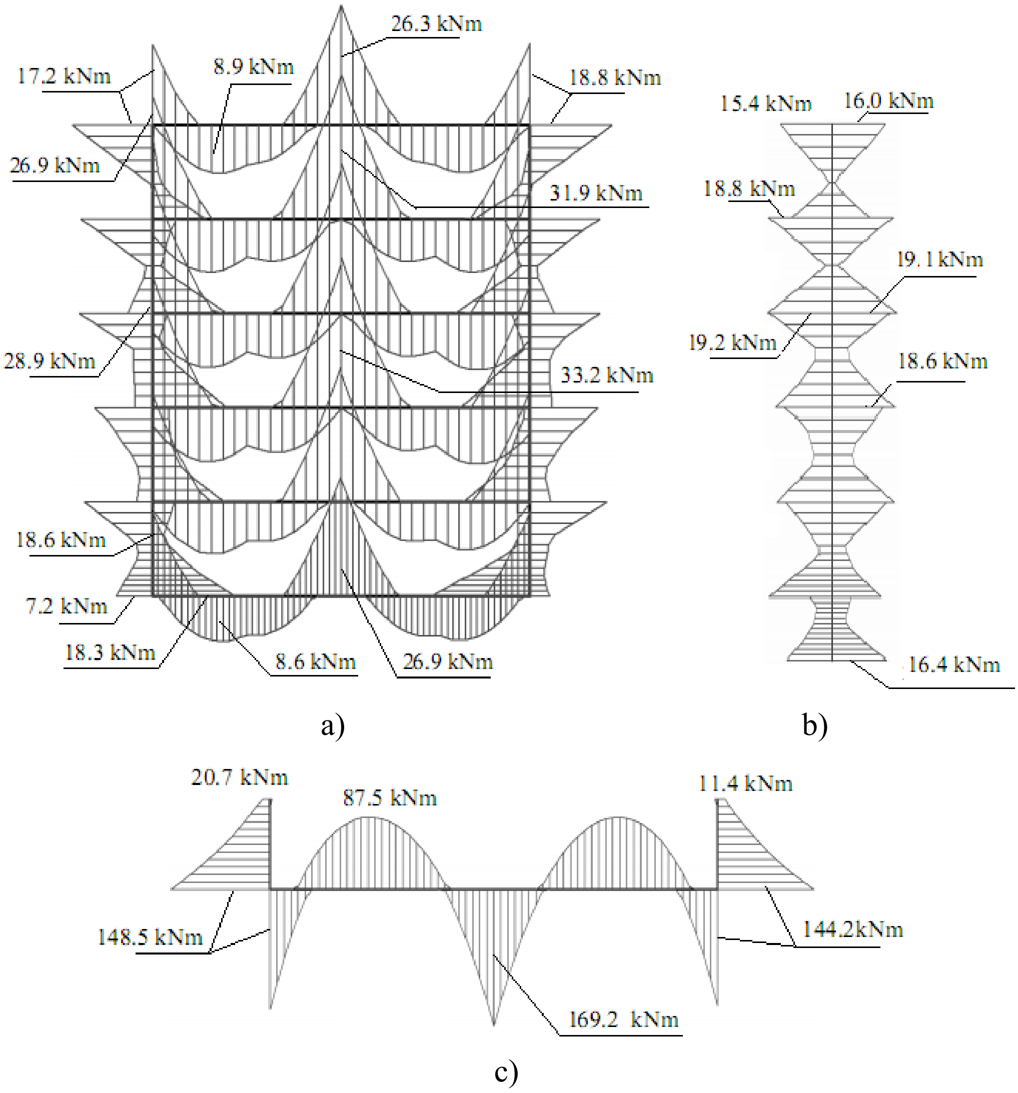

Figure 13: Plot of envelopes of bending moment in case of HS soil model:
a – in frame, b-in middle wall, c – in basement

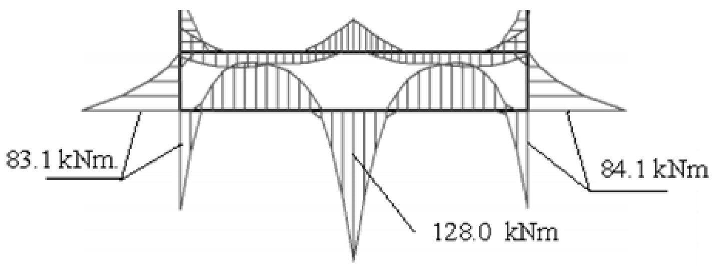

Figure 14: Plot of envelopes of bending moment in flexible basement for HS model

3.2 Seismic action on retaining wall

The studied object represents a cantilever tee retaining wall and contact soil massive 40 m in length and 14 m in height without groundwater (Fig. 15). Cantilever tee retaining wall made of reinforced concrete, the height of the vertical wall is 4.30 m, horizontal slab width is 4.50 m, wall and slab thickness is 0.2 ÷ 0.4 m. Soil massive consists of uniform sand layer, which is modelled as LE, MC and HS, geotechnical soil parameters are presented in table 4. Reinforced concrete wall slab is modelled with constant elasticity along the length and height parameters, material properties of the retaining wall are presented in table 4. Control point A – on the top of wall, B – on the bottom of wall, C – on the bottom of mesh.

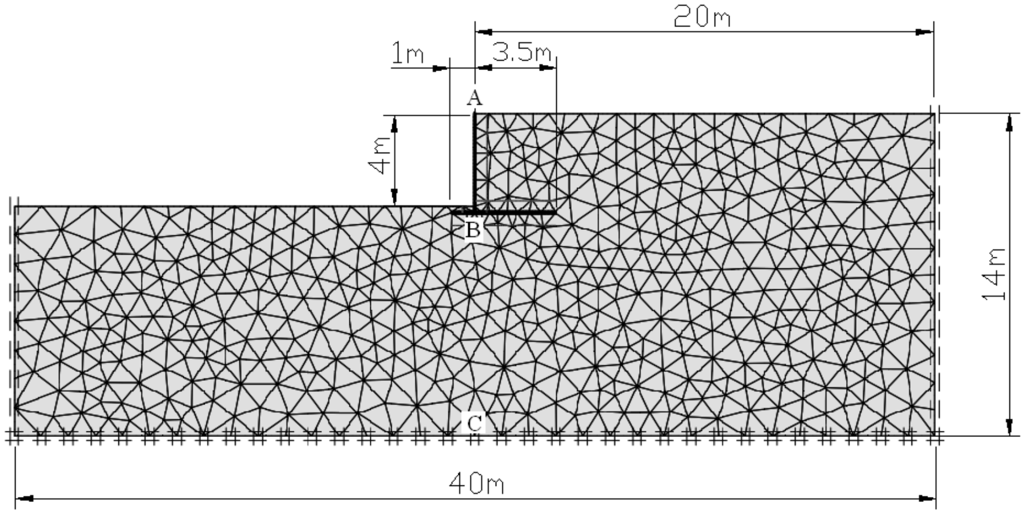

Figure 15: Finite element mesh and geometry of retaining wall

Parameter	Unit	Name	Sand	Sand	Sand
Material model	-	model	LE	MC	HS
Unit weight above p.l.	kN/m^3	γ_{unsat}	18	18	18
Young's modulus	kN/m^2	E	30000	30000	
Stffness parameters	kN/m^2	E^{ref}_{50}			30000
	kN/m^2	E_{oed}^{ref}	-	-	30000
	kN/m^2	E_{ur}^{ref}	-	-	60000
Power	-	m	-	-	0.5
Poisson's ratio	-	ν	0.2	0.2	0.2
Cohesion	kN/m^2	c_{ref}	-	0.1	0.1
Friction angle	o	φ	-	30	30
Dilatancy angle	o	ψ	-	0	0
Rayleigh damping	-	α_R, β_R	0.01	0.01	0.01

Table 4: Geotechnical soil parameters

In Fig. 16 time - acceleration curves and in Fig. 17 time-displacement curves are presented for point A for all types of soil models. Plots in Fig. 18, 19, 20 show respectively time – acceleration, time – velocity and time-displacement curves for control points A and C in case of LE soil models. The acceleration for points A and B coincides because of rigidity of wall.

Parameter	Unit	Name	Wall/plate
Material model	-	model	elastic
Normal stiffness	kN/m	EA	$8.1 \cdot 10^6$
Flexural rigidity	kNm^2/m	EJ	$6.075 \cdot 10^4$
weight	kN/m/m	w	7.5
Poisson's ratio	-	ν	0
Rayleigh damping	-	α_R, β_R	0.01

Table 5. Material properties of the retaining wall

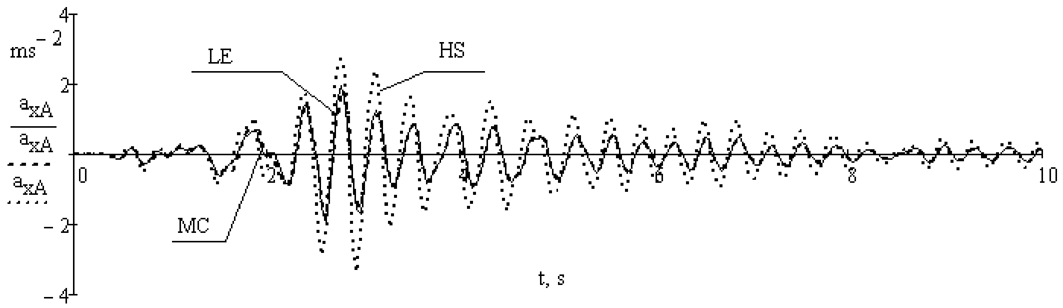

Figure 16: Time-acceleration curves of point A in case of LE MC HS model

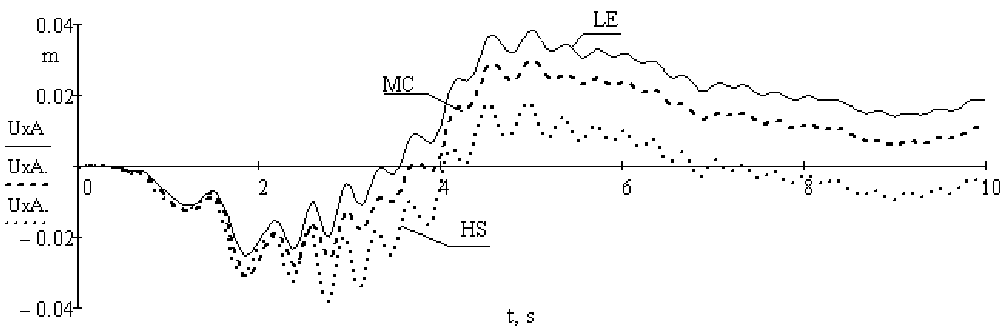

Figure 17: Time-displacement curves of point A in cases of LE MC HS model

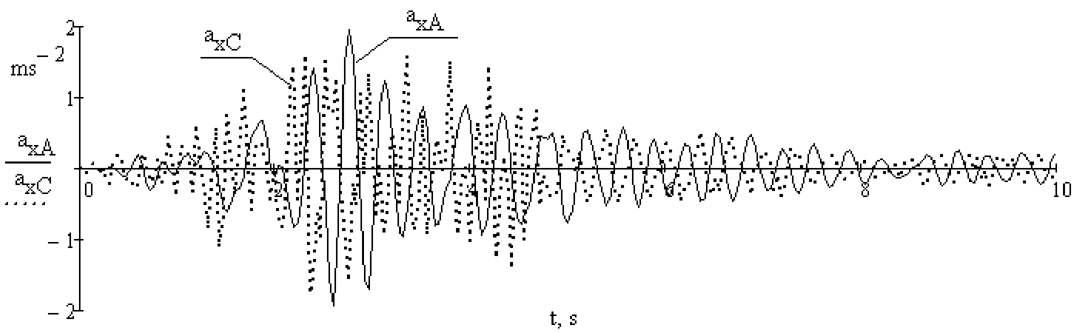

Figure 18: Time-acceleration curves of points A and C in case of LE model

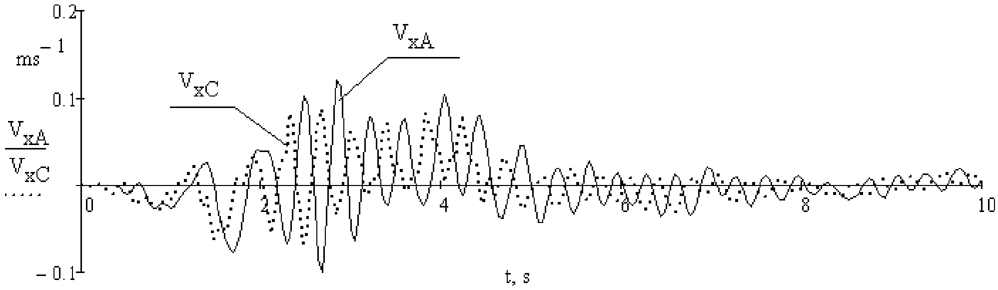

Figure 19: Time - velocity curves of points A and C in case of LE model

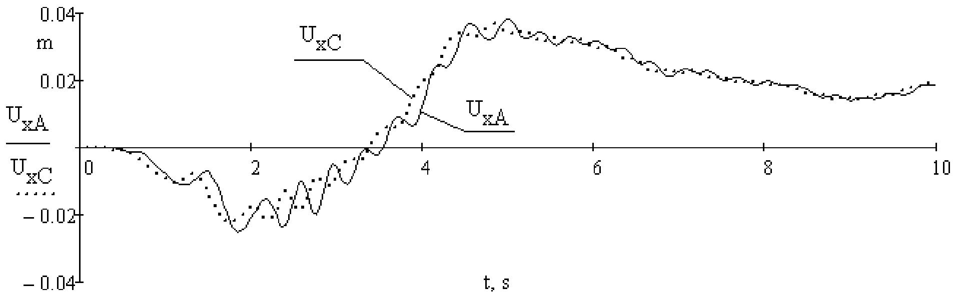

Figure 20: Time-displacement curves of points A and C in case of LE model

Soil model	A				B				C			
	Displac-ement		Accelera-tion		Displase-ment		Accelera-tion		Displase-ment		Accelera-tion	
	u_{max} mm	t, s	a_{max} ms^{-2}	t, s	u_{max} mm	t, s	a_{max} ms^{-2}	t, s	u_{max} mm	t, s	a_{max} ms^{-2}	t, s
LE	38	5.0	1.93	2.76	38	4.96	1.49	2.56	37	4.84	1.76	2.36
MC	35	5.0	1.84	2.60	34	4.96	1.44	2.56	37	4.84	1.76	2.36
HS	38	2.76	3.34	2.96	27	1.80	1.73	2.84	37	4.84	1.76	2.36

Table 6. Maximal value of parameters of vibration in control points A, B, C

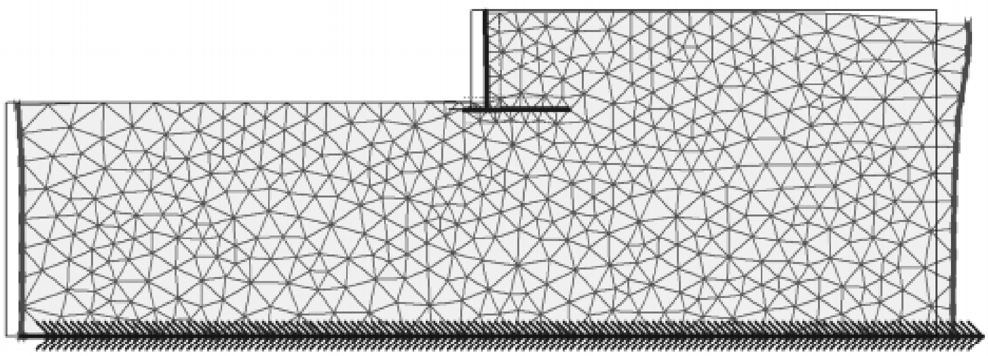

Figure 21: Deformed mesh of MC at t= 5.0 s max horizontal displacement 34 mm

In table 6 maximum values of vibration parameters of control points are given.
Fig. 21 shows the deformed mesh and maximum horizontal deformation at wall top.

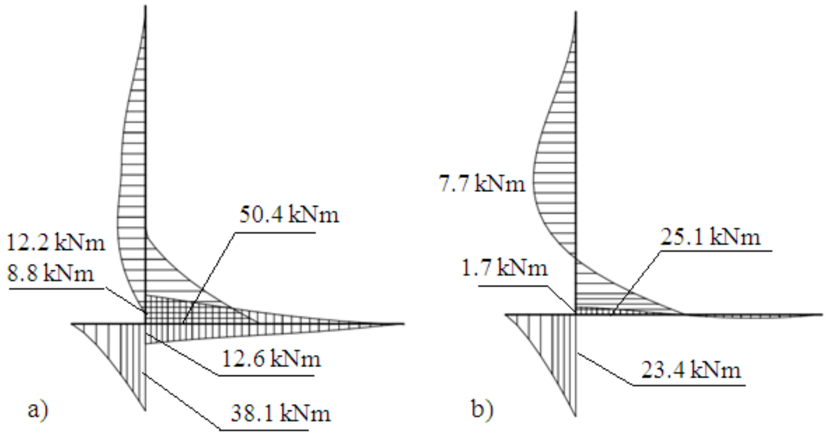

Figure 22: Bending moments diagram for LE soil model: a) envelopes of bending moment, b) static bending moment

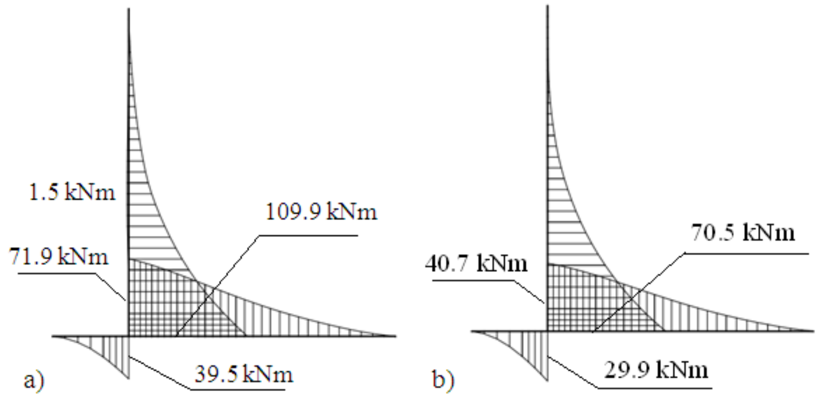

Figure 23: Bending moments diagram for MC soil model: a) envelopes of bending moment, b) static bending moment

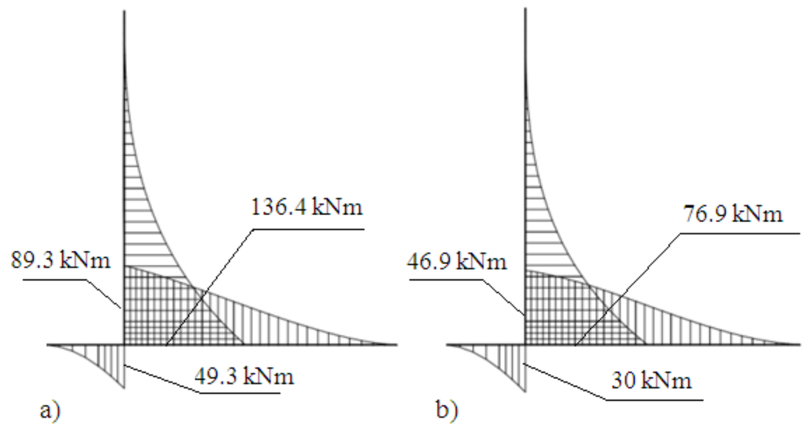

Figure 24: Bending moments diagram for HS soil model: a) envelopes of bending moment, b) static bending moment

In Fig.22÷24 the envelopes of bending moment under the seismic action and static bending moments are presented for every soil model. It is obvious that bending moments differ significantly.
Check the active pressure of the soil on the retaining wall in the case of vertical wall surface and horizontal ground level is fulfilled in accordance with [6]. In accordance with classical theory static active soil pressure as linear function of *z*:

$$q_a(z) = \gamma \cdot z \cdot \frac{1 - \sin\varphi}{1 + \sin\varphi} = \gamma \cdot z \cdot 0.333 = 6z$$

Static bending moment in the wall:

$$M(z) = \frac{1}{2} q_a(z) \cdot z \cdot \frac{1}{3} \cdot z$$

and on the depth 4.30m (the middle of the plate) is:

$$M(z) = \frac{1}{2} q_a(z) \cdot z \cdot \frac{1}{3} \cdot z = z^3 = 4.3^3 = 79.5kNm$$

Here passive soil pressure on depth 0.3 m may be neglected.
For seismic active soil pressure
The friction angle should to be decrease on the seismic angle λ:

$$\lambda = arctg\frac{a}{g}$$

which is equal to *10.96°,* if seismic acceleration *a* is assumed equal to $1.90\ m/s^2$.
If specific gravity of soil is assumed $\gamma/cos(\lambda)$, than seismic pressure on the retaining wall is:

$$q_{as}(z) = \gamma \cdot z \cdot \frac{1}{\cos^2\varphi}\left[1 - \sqrt{\frac{\sin(\varphi - \lambda) \cdot \sin\varphi}{\cos(\lambda)}}\right]^2 = \gamma \cdot z \cdot 0.468 = 8.422z$$

Dynamics bending moment in the wall on depth 4.30m:

$$M(z) = \frac{1}{2} q_{as}(z) \cdot z \cdot \frac{1}{3} \cdot z = 1.404 \cdot z^3 = 1.404 \cdot 4.3^3 = 111.7kNm$$

For HS model the maximal acceleration is equal 3.34m/s^2, $\lambda = 18.8°$ seismic pressure and bending moment:

$q_{as}(z) = \gamma \cdot z \cdot 0.616 = 11.09z \qquad M(z) = 1.848 \cdot z^3 = 1.848 \cdot 4.3^3 = 146.96kNm$.

Elastic vibration of concrete wall may be neglected, taking into account its massiveness and additional moment of inertia forces may be assumed as:

$$\Delta M(z) = ma \cdot z^2 \frac{1}{2} = 0.75 \cdot 2 \cdot 4.3^2 = 13.9kNm$$

It may be concluded that MC soil model reflect the behavior of wall sufficiently enough. LE soil model shows the unrealistic results in static stage – small bending moment in the vertical wall, and envelopes of dynamics bending moment may be twice underestimated.

3.3 Seismic action on dam

In this chapter the river embankment under seismic action is considered. Embankment (Fig.25) is 5 m high and consists of impervious clay. The upper 6 m of the subsoil consists of soft soil layer, of which the top 3 m is modeled as a clay layer and the lower 3 m as a peat layer. Bellow the soft soil layers there is a deep permeable sand layer, of which the upper 9.0 m are included in the finite element model. It is assumed, that the water in the sand layer is in the contact with the river. Soil massive included in the geometry is 120m in horizontal direction and 20m in vertical direction, control points location is shown in Fig.25. Soil properties are presented in table 7, here the LE and MC soil model are investigated because of absence valid laboratory data of HS model of soft soil.

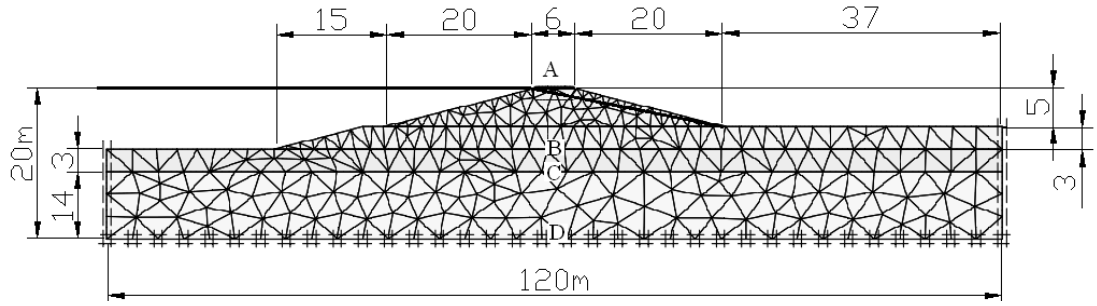

Figure 25: Finite element mesh and geometry of dam

Parameter	Unit	Name	Clay	Peat	Sand
Material model	-	model	MC	MC	MC
Type of behaviour	-	type	undrain	undrain	drain
Unit weight above p.l.	kN/m^3	γ_{unsat}	16	13	17
Unit weight below p.l.	kN/m^3	γ_{sat}	18	16	20
Horizntal permeability	m/day	k_x	0.001	0.01	1.0
Verical permeability	m/day	k_y	0.001	0.001	1.0
Young's modulus	kN/m^2	E_{ref}	12000	3000	26000
Poisson's ratio	-	ν	0.35	0.35	0.3
Cohesion	kN/m^2	c_{ref}	36	7	2
Friction angle	^{o}	φ	12	20	28
Dilatancy angle	^{o}	ψ	-	0	0
Rayleigh damping	-	α_R , β_R	0.015	0.015	0.015

Table 7. Material properties of embankment and subsoil

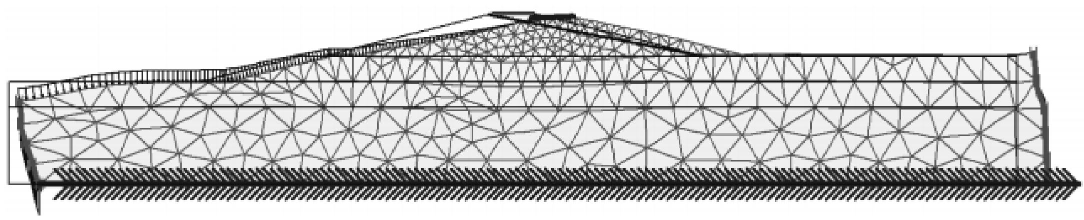

Figure 26: Deformed mesh for MC soil model at t=4.8s, maximal horizontal displacement U_{xA}=46mm

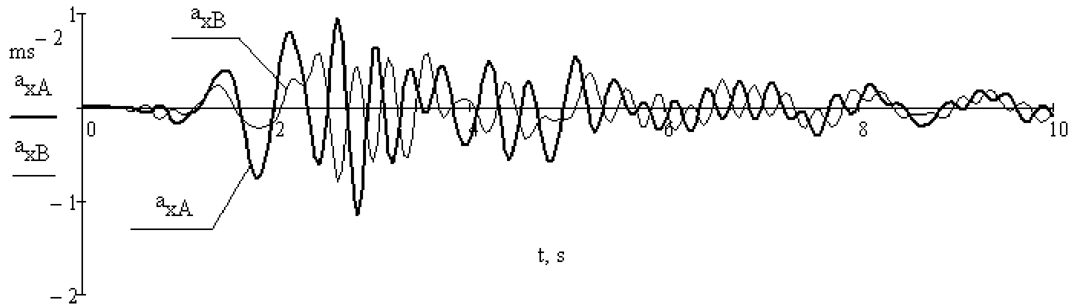

Figure 27: Horizontal acceleration of soil particles in points A and B for MC model

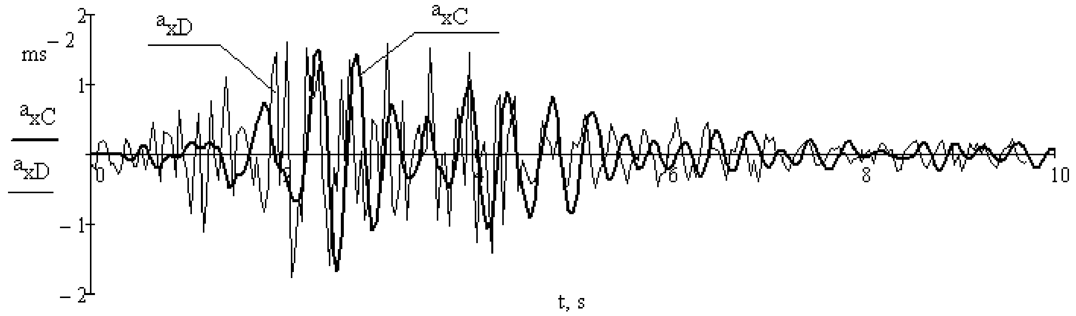

Figure 28: Horizontal acceleration of soil particles in points C and D for MC model

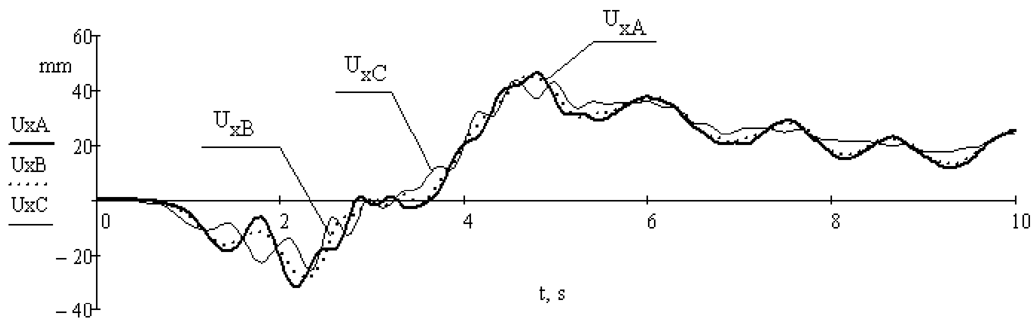

Figure 29: Horizontal displacements of soil particles in points A, B, C for MC model

Soil model	A				B				C			
	Displac-ement		Accelera-tion		Displase-ment		Accelera-tion		Displase-ment		Accelera-tion	
	u_{max} mm	t, s	a_{max} ms^{-2}	t, s	u_{max} mm	t, s	a_{max} ms^{-2}	t, s	u_{max} mm	t, s	a_{max} ms^{-2}	t, s
LE	45	4.80	1.23	2.84	42	4.68	0.79	2.64	40	4.56	1.79	2.64
MC	46	4.76	1.15	2.84	45	4.72	0.80	2.64	44	4.56	1.94	2.56

Table 8. Maximal parameters of soil particles vibration in control points A, B, C

In table 8 maximum values of soil vibration parameters in control points are given. Fig. 26 shows the deformed mesh and maximum horizontal deformation of the top of dam. In fig.27 horizontal acceleration of soil particles in points A, B and in Fig. 28 of points C, D dependence on time during seismic action are presented for MC model. Fig. 29 shows horizontal displacements of soil particles in points A, B, C for MC soil model.
In the absence of contacting with soil structural elements of both soil model gives the identical results.

4 Conclusion

The results of numerical modeling of engineering constructions behavior depending on the subsoil properties under action of seismic loading are presented in this work. The comparison of three soil models linear-elastic, Mohr-Coulomb and hardening soil is executed for three types of engineering constructions subject to an earthquake: five- storey building, retaining wall and river embankment.
As a result of the calculations displacements, velocities and accelerations of control points on structures elements and in the soil (dependent on time) were obtained; the internal forces in the structural elements are determined. The results are different for every soil model; some results are compared with existing recommendations and this comparison demonstrates the coincidence with the MC model results.

Acknowledgments

This work has been supported by the ERDF's grant, within the project "SATTEH", No 2010/0189/2DP/2.1.1.2.0/10/APIA/VIAA/019, being implemented in Engineering Research Institute "Ventspils International Radio Astronomy Centre" of Ventspils University College (VIRAC).

References

[1] R .W. Clough, J. Penzien, Dynamics of Structures. New-York, 1975.
[2] Wang, J.-N. "Seismic design of tunnels: A state-of-the-art approach". Monograph 7. Parsons, Brinckerhoff, Quade and Douglas Inc., 1993.
[3] Hashash, Y.M.A., Hook, J.J., Schmidt, B., Yao J.I-C., "Seismic design of underground structures". Tunnelling and Underground space technology 16/4, 2001, 247-293.
[4] Plaxis b.v. Delft, the Netherland, 2007.
[5] G.M. Lomidze, "Calculation of retaining walls on seismic stability", in collected papers "Earthquake Engineering" Transcaucasian State Publishing House, 1931.